



Predicting land subsidence rate due to groundwater exploitation in the district 19 of Tehran using MODFLOW and InSAR

Mojtaba Arjomandi¹, Ali Saremi^{2*}, Amirpouya Sarraf³, Hossien Sedghi⁴ and Mahasa Roustaei⁵

¹Ph.D. Student, Department of Water Sciences and Engineering, Science and Research Branch, Islamic Azad University, Tehran, Iran

²Assistant Professor, Department of Water Sciences and Engineering, Science and Research Branch, Islamic Azad University, Tehran, Iran

³Assistant Professor, Department of Civil Engineering, Roudehen Branch, Islamic Azad University, Roudehen, Iran

⁴Professor, Department of Water Sciences and Engineering, Science and Research Branch, Islamic Azad University, Tehran, Iran

⁵Assistant Professor, Geological Survey of Iran, Tehran, Iran

ARTICLE INFO

Received: 2017 November 02

Accepted: 2017 December 30

Available online: 2018 March 17

Keywords:

Groundwater

InSAR

Land subsidence

MODFLOW

*Corresponding author:

A. Saremi

E-mail: iranma4@gmail.com

ABSTRACT

During recent years, groundwater exploitation and thereby decreasing hydraulic head in the compressible sedimentary aquifer which is placed in the district 19 of Tehran have been caused noticeable land subsidence. The land subsidence has been damaging the infrastructures which have been being built in the south of Tehran Basin, especially in the district 19 of Tehran. A finite-difference groundwater flow model (MODFLOW) and a synthetic aperture radar (SAR) method have been used to estimate and predict the rate of land subsidence in this area, and help hydrogeologists manage the vital groundwater resource correctly. The data have been imported into the model, and the change of the amount of land subsidence and head have been obtained for 39 years. Then the available radar images have been processed. Afterwards, the head calibration and subsidence calibration have been done. The results of the calibrations confirmed the accuracy of the results obtained by the model. Finally, this study suggests that 118 mm of land subsidence and an 11.6 m piezometric head decline are likely to occur from 2014 until 2043.

1- Introduction

In the south of Tehran plain, groundwater has been being used as a vital water resource for some purposes; such as, industrial, domestic, agricultural and residential uses. Moreover, due to population growth, pollution of groundwater and land subsidence in the south of Tehran Plain, the management of the resource is so important. The following table (or table 1) shows some previous pumping-induced land subsidence studies.

The main purpose of this paper is to predict the amount of pumping-induced land subsidence due to the decrease of piezometric head in the aquifer, located in the Quaternary sediments of Kahrizak Formation, using InSAR and MODFLOW.

2- Initial material and data

Initial hydraulic head changes have been measured since 2008 to 2016. Hydraulic conductivity has been measured in a well under study using aquifer test. MODFLOW code

(Simcore 8) which is a free version has been used to estimate the amount of land subsidence in the future. SAR images for three years (2014, 2015 and 2016) which have been bought by Geological Survey of Iran (GSI) have been used. Moreover, these images cover the district 19 of Tehran. After image processing, the amount of land subsidence for each of the years has been determined. Effective porosity which is equal to specific yield for the confined aquifer and the confining aquifer has been measured in a laboratory. The average thickness of the confined aquifer and the confining aquifer has been used in MODFLOW. The depth of wells has been assumed as the depth of the aquifer's bedrock. In addition to, in this paper, we have assumed that the aquifer is homogenous.

3- Geology and the hydrogeology settings of this area

Tehran basin is an arid to semi-arid region with the area of 2250 km². Its annual precipitation is about 200 mm.

Table 1- Previous studies on the rate or amount of land subsidence due to groundwater exploitation

Reference	Previous studies
Sun et al. (1999)	Land subsidence due to groundwater exploitation and sea level rise in New Jersey, the USA using InSAR (the rate of land subsidence is equal to 3 cm/year)
Tosi et al. (2009)	Considering the rate of land subsidence in Venice using InSAR (the rate of land subsidence is equal to 1.4 cm/year)
Chang et al. (2004)	Considering the rate of land subsidence using InSAR in Taiwan (the rate of land subsidence is equal to 3 cm/year)
Carbognin et al. (2004)	Considering the rate of land subsidence using InSAR in Venice Lagoon (the rate of land subsidence is between 3 to 5 cm/year)
Phien-Wej et al. (2006)	Considering the rate of land subsidence using InSAR in Japan coasts (the rate of land subsidence is equal to 4 cm/year)
Hayashi et al. (2009)	Considering the rate of land subsidence using InSAR in Bangkok coasts (the rate of land subsidence is equal to 12 cm/year)
Leake and Galloway (2010)	Estimating the rate of land subsidence in Antelope Valley, California (the amount of land subsidence is equal to 2 m from 1992 to 1930)
Calderhead et al. (2011)	Estimating the rate of land subsidence in Toluca, Mexico using InSAR (the amount of land subsidence is equal to 2 m from 1965 to 2009)
Erban et al. (2014)	Considering the rate of land subsidence using InSAR in the Mekong Delta, Vietnam (the rate of land subsidence is equal to 3 cm/year)
Mahmoodpour et al. (2015)	Considering the rate of land subsidence using InSAR and MODFLOW in Shahriar, Iran (the rate of land subsidence is equal to 33 cm/year)

Its annual evaporation is about 2500 mm (Calderhead et al., 2011). Its topography is mild-slope. Its temperature usually changes from 0 to 45 °C. Noticeable pumping-induced land subsidence observes in the south, southwest and southeast of Tehran Plain (Molaei et al., 2016). The area of the studied land subsidence region (or the district 19 of Tehran) is about 60 km². Besides, the longitude and the latitude of the center of the studied area are 51.3° E and 35.6° N respectively. Figure 1 shows the location of the studied area and the land subsidence area.

The alluvial aquifer of the area is comprised of silt, fine sandstones with a lot of clay interbeds. Alluvial deposits of Tehran consist of four stratigraphic units: A (Hezardarreh formation), B (Kahrizak formation, Qt1), C (Tehran alluvial formation, Qt2), and D (recent alluvium) (Darvishzadeh, 2006).

The ancient alluvial deposits of Hezardarreh formation comprise conglomerates with a few lenses of sandstone, siltstone and mudstone. The thickness is estimated to be about 1200 m. Besides, the oldest rock outcrops in the study area are represented by tuff, andesitic and pyroclastic rocks of the Eocene age. Hezardarreh formation is an impermeable rock unit with extensive cementation and high compaction (Molaei et al., 2016). The Kahrizak formation is a heterogeneous early Quaternary formation which forms a flat-layering sheet of alluvial sediment outcropping between the Hezardarreh anticlinal folds and the Alborz margin. This formation consists of clayey silt. The thickness of the Kahrizak formation is uncertain in the southern region of Tehran plain (Darvishzadeh, 2006). Faulting has affected the formation in many places; however, it lays horizontally without tilting. Tehran alluvium (the C unit) refers to the

sub-recent alluvium of the late Quaternary deposits that have been exposed between the Alborz and anti-Alborz. Also, it consists of silty loam deposits predominantly. Moreover, the thickness of this formation is uncertain in the southern region of Tehran plain. The age of the Tehran alluvial formation is estimated to be 50,000 to 10,000 years (late Pleistocene). The D Unit is the youngest stratigraphic unit in the Tehran region and presents as alluvial and fluvial deposits (Darvishzadeh, 2006). This unit is composed of fine silt. Moreover, Tehran alluvium and the Kahrizak formation represent potential aquifers with good hydraulic conductivity (Calderhead et al., 2011). In addition to, in this paper, we have assumed that no tectonic action has been occurring while the amount of land subsidence has been being estimated and predicted.

Hydrogeological units of the district 19 of Tehran are divided to three aquifers and three aquitards. Besides, the water quality of the lower aquifer is in the allowable limit (TDS < 4 gr/L) (Calderhead et al., 2011). The thickness of the lower aquifer is 24 m. Moreover, a thick aquitard with the thickness of 31 m is lying on the lower aquifer (Calderhead et al., 2011). In addition to, in this paper, we ignored the amount of elastic storage due to it is less and the Hydrogeological units of the studied area are inelastic (or plastic). Also, annual average subsidence rates, with the declining trend in hydraulic heads, have been being considered. As well as, horizontal deformation has been being ignored.

4- Methodology and discussion

In this study, MODFLOW (SIMCORE 8) which is a free version and GAMMA software (for SAR image processing)

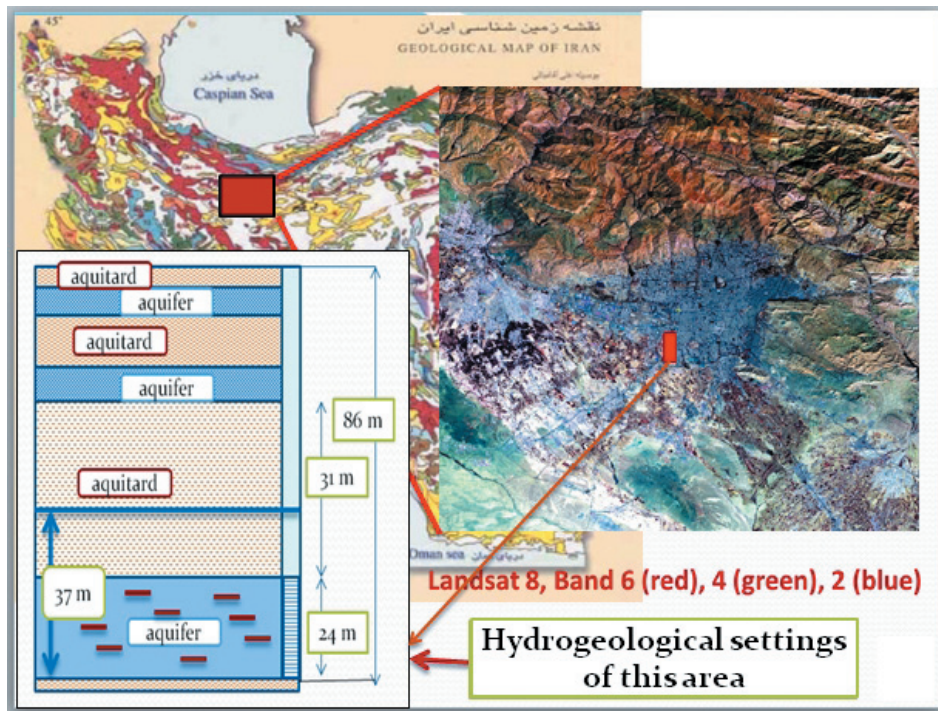


Fig. 1- The above figure Shows the study area and the hydrogeological setting of the district 19 of Tehran. Besides, the aquifers have been shown using blue color, and aquitards have been shown using brown color. The right image is Landsat 8 (band 6 4 2). The district 19 of Tehran (the area of land subsidence) has been shown as a red rectangle in the right map (Landsat 8). The longitude and the latitude of the center of the area are respectively 51.3° E and 35.6° N Brown horizontal lines in the lower aquifer show clay interbeds. Besides, the upper right figure shows the map of Iran, and the red rectangle which is placed or marked in it shows the area of Tehran Watershed Basin.

which has been bought by Geological Survey of Iran are used to estimate and predict the amount of land subsidence from 2008 to 2043. MODFLOW uses version 1 of Interbed Storage Package (IBS1) to calculate and predict the amount of compressibility in each cell of the model due to groundwater exploitation. IBS1 which has been developed by Leake and Prudic in 1991 uses a simple formula based on Terzaghi's effective stress principle (Carbognin et al., 2004; Ferretti et al., 2007; Mahmoodpour et al., 2015).

4- 1. MODFLOW method

The principle assumes that (1) a unit decrease in head causes a unit increase in effective stress, and (2) the characteristics of skeletal storage are not related to the effective stress. In IBS1, if the present hydraulic head is more than the preconsolidation head, there is elastic storage and a decrease in elastic storage causes elastic compressibility. On the other hand, in IBS1, if the present hydraulic head is less than the preconsolidation head, there is inelastic (or plastic) storage and a decrease in inelastic storage causes inelastic compressibility. In addition to, IBS1 assumes that the equilibration of hydraulic head between clay interbeds (or low permeability units) and the adjacent aquifer happens

immediately and so fast. When the aquifer is inelastic, or recent hydraulic head is less than the preconsolidation head (inelastic storage is predominant), the following equation is used (Carbognin et al., 2004; Ferretti et al., 2007):

$$\Delta b = S_s * b * \Delta h$$

In the above relation, $\Delta b [L]$ is the change in the thickness of a layer. $S_s [1/L]$ is specific storage. $b [L]$ is the initial thickness of the layer. $\Delta h [L]$ is the change in hydraulic head.

Other relations which have been used in IBS1 will be mentioned at appendices. Also, more detail information about the relations (or equations) can be found in Erban et al. (2014), Calderhead et al. (2011), Leake and Galloway (2010), Chang et al. (2004).

Also, in all parts of the critical area which has been shown with red color in figure 4 (e), the amount of hydraulic head drawdown in all cells are the same as each other due to there is a composite drawdown curve for all the wells being pumping (or a resulting cone of depression has been caused by all wells being pumped in the critical area (or the phenomena of the cone of depression interference)).

Moreover, the pumping rate from each of the wells is at least equal to 258 m³/day. The initial hydraulic head is

equal to 3700 cm in 2008. Moreover, in the critical area, hydraulic head reduces between 30 to 45 cm during every year (Calderhead et al., 2011). Although, during a few years, hydraulic head has increased, the hydraulic head changes have showed a decrease trend since 2008 to 2016. The longitude and the latitude of the center of the studied area are respectively 51.3° E and 31.6° N. The studied area has been divided into 800 cells. The length and the width of each cell are equal to 300 m. The groundwater quality of the lower aquifer is in a permissible limit; besides, the amount of TDS is less than 400 mgr/lit in the lower aquifer. The slope of the bedrock, based on the depths of wells, is about 0.008. The number of nodes is equal to 3200. The lower aquifer, placed in Kahrizak Formation of Quaternary age, consists of deposits of siltstone, fine sandstone and a lot of clay interbeds. Besides, upper and

lower bounds are constant flux boundaries. Also, eastern and western bounds are parallel to the hydraulic gradient trend, so that no flow boundaries are assigned with them. Also, the period length of stress which is imposed to the aquifer is equal to $9.0015E+07$ sec. Besides, the number of time steps is equal to 120. In addition to, in this model, transient flow has been selected. The average depth in this model is equal to 86 m. Also, the slope of hydraulic gradient is approximately more than the slope of the bedrock. The horizontal hydraulic head of the aquitard is equal to 1.4×10^{-6} m/sec. Also, the horizontal hydraulic head of the confining aquifer (the lower aquifer) is equal to 2.6×10^{-5} m/sec. The vertical hydraulic conductivity of the confining aquifer is 1.6×10^{-6} m/sec. The vertical hydraulic conductivity of the aquitard (the confined aquifer) is equal to 1.6×10^{-7} m/sec. The leakage factor or (β) of the aquitard is equal to

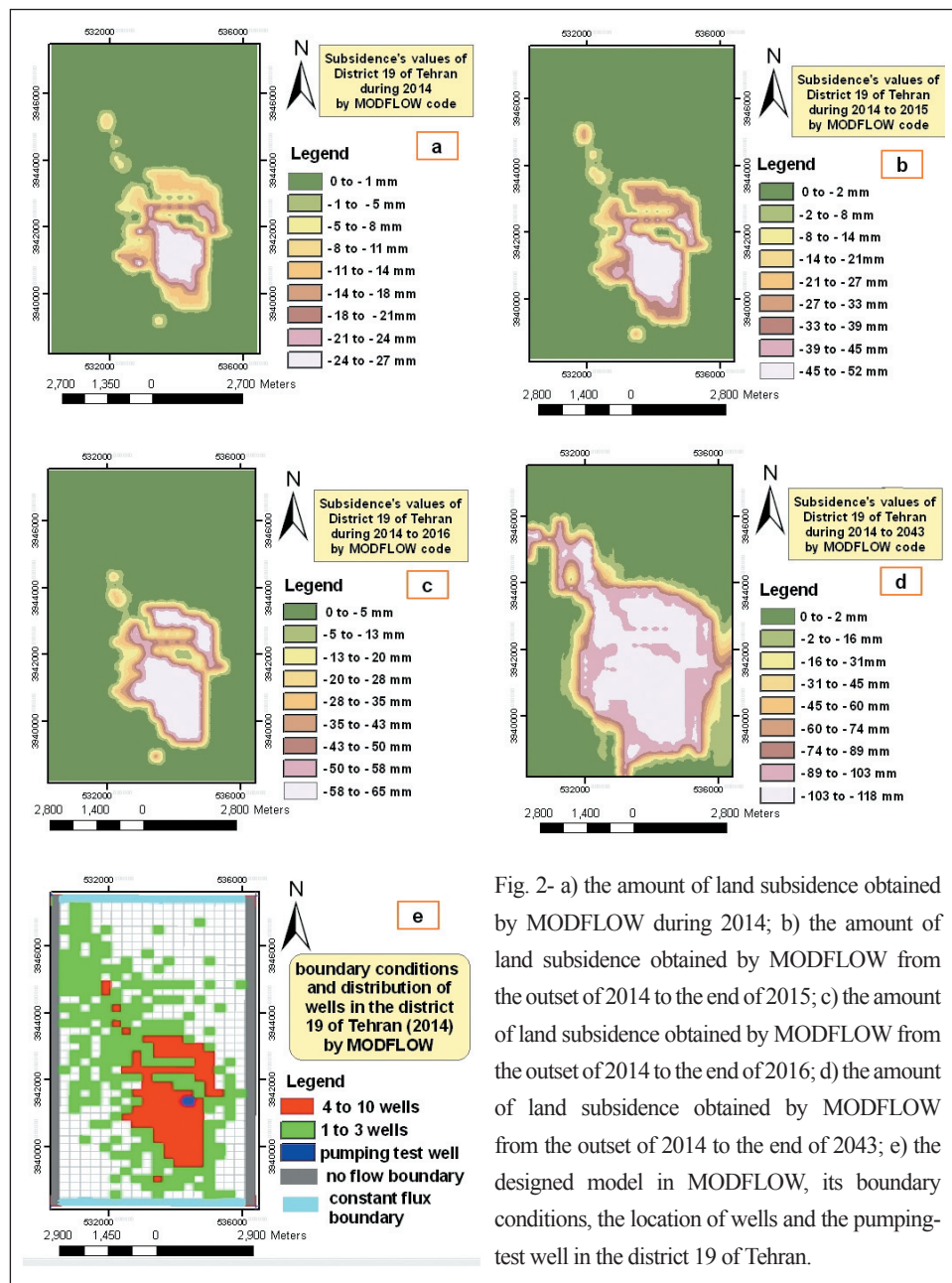


Fig. 2- a) the amount of land subsidence obtained by MODFLOW during 2014; b) the amount of land subsidence obtained by MODFLOW from the outset of 2014 to the end of 2015; c) the amount of land subsidence obtained by MODFLOW from the outset of 2014 to the end of 2016; d) the amount of land subsidence obtained by MODFLOW from the outset of 2014 to the end of 2043; e) the designed model in MODFLOW, its boundary conditions, the location of wells and the pumping-test well in the district 19 of Tehran.

$2.8 \cdot 10^{-8} \text{ m/sec}$. The amount of the leakage factor is defined using the following formula:

$$\beta = K_v / L$$

In the above formula, K_v is vertical hydraulic conductivity. Moreover, L is the thickness of the confining aquifer (aquitar). Besides, the average thickness of the confined aquifer (or the aquitar) is equal to 32 m . The effective porosity of the confining aquifer is approximately equal to 0.1 . Moreover, for the confined aquifer (or the lower aquifer), the effective porosity is approximately equal to 0.25 based on the samples which have been tested in a laboratory. The average rate of precipitation is equal to 200 mm/year . Also, in this model, the amount of $6 \cdot 10^{-6} \text{ mm/sec}$ has been assigned to each of the cells.

At the end, the model is able to estimate and predict the amount of outputs, i.e. the amount of hydraulic head and compressibility (or land subsidence) for every year. Based on the relations that this model is used in itself, the amount of land subsidence during 2014 is equal to 27 mm . Besides, the amount of land subsidence during 2014 and 2015 is equal to 52 mm . Moreover, the amount of land subsidence from the beginning of 2014 to the end of 2016 is equal to 65 mm . Besides, the amount of land subsidence the beginning of 2014 to the end of 2043 is equal to 118 mm .

The calibration of head between the data which have been obtained by the model and the field data which have been measured since 2008 to 2016 has been done. The head calibration is shown in the following figure (fig. 3):

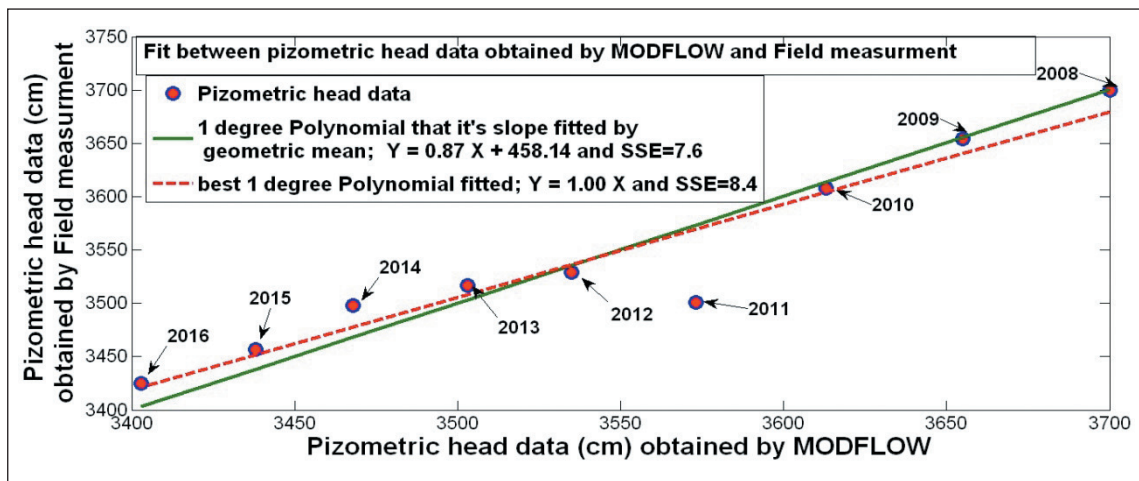


Fig. 3- Head calibration between the piezometric head data measured in the field and the piezometric head data obtained by MODFLOW.

4- 2. Synthetic aperture radar method

Field measurements of subsidence rates are only useful for small-scale areas. Also, remote sensing observations are necessary to monitor and consider land deformation in large-scale regions precisely.

In this approach, land deformation or surface displacement is determined along the radar line of sight by measuring a phase difference between master and slave images (based on image acquisition wavelengths). In SAR observations, two different radar imaging geometries are there:

- (1) ascending passes (the radar goes from South to North) and
- (2) descending passes (the radar goes from North to South) (Hayashi et al., 2009). Also, the SAR antenna (or the radar antenna) is always pointed to the right side of the track for ERS and Envisat. Thus, the same scene on the ground is observed by the SAR antenna from the east during the

descending passes and from the west during the ascending passes (Hayashi et al., 2009). Moreover, an interferogram obtained from ascending passes can be different to the other obtained from descending passes. Besides, orbital, topographic and atmospheric effects and other noises which have been there in radar images cause lack of correlation between a pair of selected images during image processing (Roustaei, 2016). Therefore, in this paper, these effects and other noises have been approximately removed using suitable and correct image processing.

For determining the amount of land subsidence rate in district 19 of Tehran (south of Tehran plain) during 2014 and 2015, COSMO-SkyMed X-band SAR images have been used; besides, during 2016, C-band Sentinel-1A SAR images have been used. Ultimately, three interferograms with time periods 20140929-20150119 (112 days), 20150129-

20150527 (128 days) and 20160611-20161220 (192 days) have been prepared using a standard image processing method. Also, the maximum rate of land subsidence after image processing is about 1 cm. The following figures (fig. 4 (a, b and c)) show the land subsidence rates during the mentioned time periods.

Moreover, the calibration of land subsidence between the data which have been obtained by the model and the data which have been measured by InSAR method since 2008 to 2016 has been done. The land subsidence calibration is shown in the following figure (figure 5).

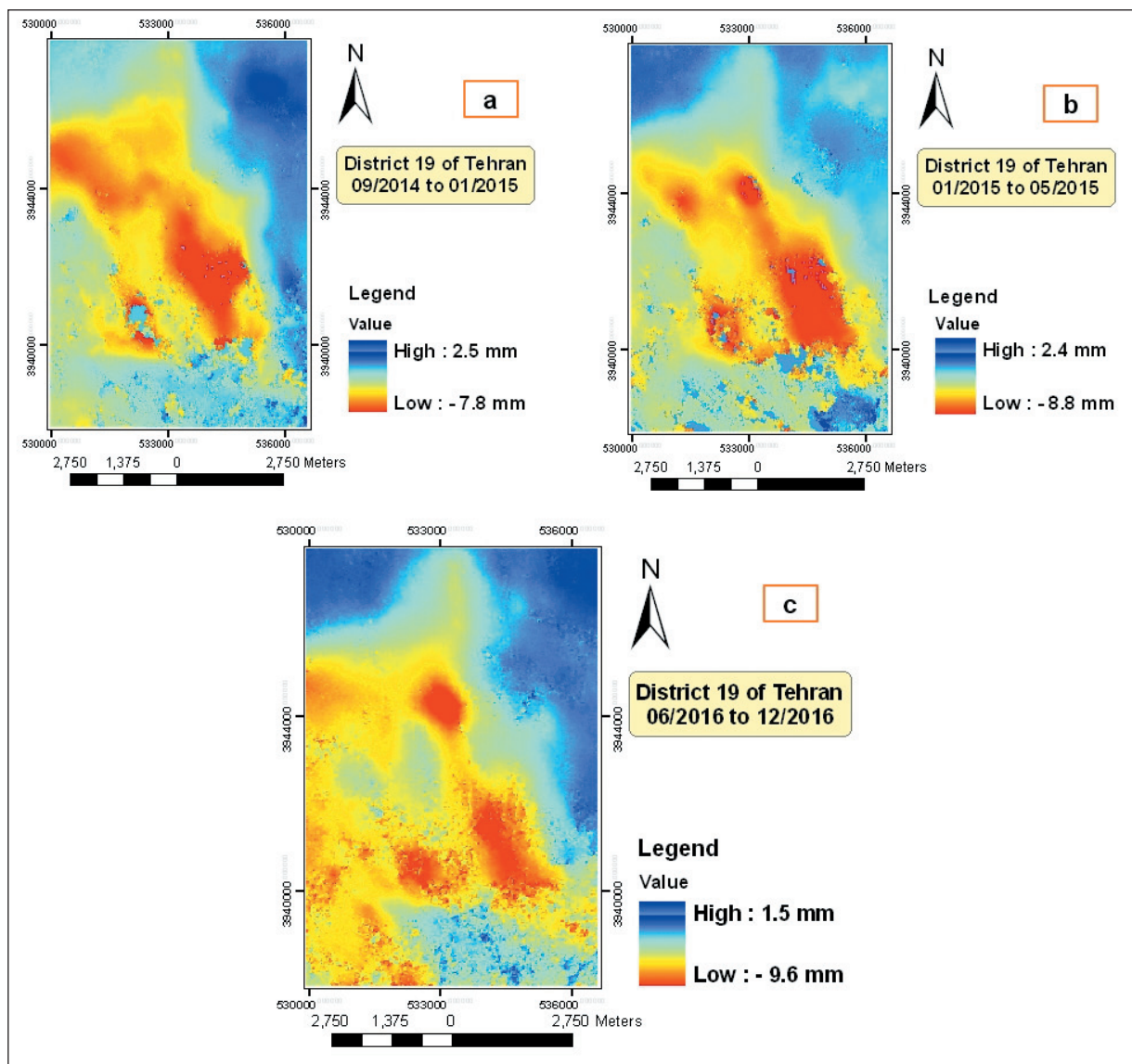


Fig. 4- The upper left corner figure; a) shows the period of land subsidence, 20140929-20150119 (112 days) using the radar image of COSMO-SkyMed4; the upper right corner figure; b) shows the period of land subsidence, 20150129-20150527 (128 days) using the radar image of COSMO-SkyMed4; the lower figure; c) shows the period of land subsidence, 20160611-20161220(192 days) using the radar image of Sentinel-1A. Also, the amount of spatial resolution is about 22.5 m in each of three interferograms.

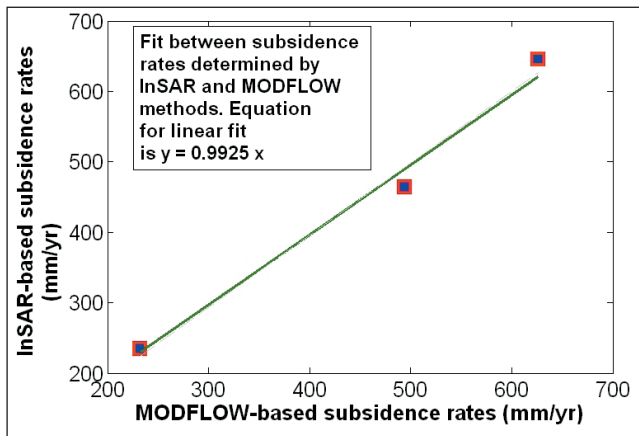


Fig. 5- Subsidence calibration between the amounts of subsidence which have been obtained by InSAR (during 2014, 2014 to 2015 and 2014 to 2016) and the amounts of subsidence which have been obtained by MODFLOW (during 2014, 2014 to 2015 and 2014 to 2016).

5- Conclusion

In this area (or the district 19 of Tehran), the phenomenon of pumping-induced land subsidence is observed. MODFLOW shows that in the area, the amount of land subsidence from 2008 to 2043 is equal to 118 mm. Moreover, the drawdown of piezometric head is equal to 11.6 m from 2008 to 2043. The head calibration between the data of piezometric head which have been measured since 2008 to 2016 and the data of piezometric head which have been obtained has been done. Besides, calibration of subsidence between the amounts of subsidence which has been obtained by MODFLOW approach and the amounts of subsidence which has been obtained by InSAR has been done. The two calibrations authenticate that the results of MODFLOW is completely correct, so that we can rely on the amounts of land subsidence which is estimated and predicted by MODFLOW. In addition to, specific storage which is a non-dimension parameter has been reduced since 2008 to 2016. Moreover, the amount of specific storage will be equal to 1.2×10^{-6} in 2043. Based on the results which have been obtained, it is obvious that the management of the groundwater resource is so indispensable. In addition to, if the decrease trend of the water budget continues or the decrease trend of piezometric head goes on, the increase trend of land subsidence goes on and the infrastructures of the area will be damaged in the future.

6- Appendices

IBS1 uses the following relations to estimate the amount of skeletal specific storage, fluid exchange and the amount of compressibility (or land subsidence):

If recent hydraulic head is more than preconsolidation head, elastic skeletal specific storage ($S_{ske} [L^{-1}]$) is calculated. Elastic skeletal specific storage is calculated using the following relation:

$$S_{ske} = (0.434 * C_r * \gamma_w) / (\sigma_{pre} * (1 + e_0))$$

If recent hydraulic head is less than preconsolidation head, inelastic skeletal specific storage ($S_{skv} [L^{-1}]$) is calculated. Inelastic skeletal specific storage is calculated using the following relation:

$$S_{skv} = (0.434 * C_c * \gamma_w) / (\sigma_{pre} * (1 + e_0))$$

In the above relations, $C_c [-]$ is an inelastic compression index, $C_r [-]$ is an elastic compression index, $\gamma_w [ML^{-3}]$ is specific gravity of water, $e_0 [-]$ is void ratio and $\sigma_{pre} [ML^{-1} T^{-2}]$ is preconsolidation stress.

The amount of volumetric fluid exchange is calculated in IBS 1 using the following relation:

$$Q = (A * b / (\Delta t_n)) * [S_{sk} * (h_n - h_{n-1}) + S_{ske} * (H_n - h_{n-1})]$$

In the above relation, $Q [L^3 L^{-3} T^{-1}]$ is the amount of volumetric fluid exchange; $A [L^2]$ is the cross-sectional area. $\Delta t_n [T]$ is the time period of the n^{th} stage. $S_{sk} [L^{-1}]$ is the skeletal specific storage. h_n is the recent hydraulic head, h_{n-1} is the hydraulic head of previous stage, $S_{ske} [L^{-1}]$ is the elastic skeletal specific storage and H_n is preconsolidation head.

The amount of elastic compressibility change ($\Delta b_e [L]$) is calculated in IBS 1 using the following relation:

$$\Delta b_e = -S_{ske} * b * \Delta h$$

The amount of inelastic (or virgin) compressibility change ($\Delta b_i [L]$) is calculated in IBS 1 using the following relation:

$$\Delta b_i = -S_{skv} * b * \Delta h$$

Acknowledgment

It is my duty to thank Professor Steven Gorelick (Stanford University), Professor Jan Ziebart (Zurich University), Akbar Javadi (Exeter University), Mr. Ali Bayatani (Geological Survey of Iran), all members of Tehran Water Resources Organization, Mr. Mostafa Arjomandi who have helped me to accomplish the study.

References

- Calderhead, A., Therrien, R., Rivera, A., Martel, R. and Garfias, J., 2011- Simulating pumping-induced regional land subsidence with the use of InSAR and field data in the Toluca Valley, Mexico," *Advances in Water Resources*, vol. 34, pp. 83-97.
- Carbognin, L., Teatini, P. and Tosi, L., 2004- Eustacy and land subsidence in the Venice Lagoon at the beginning of the new millennium, *Journal of Marine Systems*, vol. 51, pp. 345-353.
- Chang, C., Chang, T., Wang, C., Kuo, C. and Chen, K., 2004- Land-surface deformation corresponding to seasonal ground-water fluctuation, determining by SAR interferometry in the SW Taiwan, *Mathematics and Computers in Simulation*, vol. 67, pp. 351-359.
- Darvishzadeh, A., 2006- geology of Iran, Amirkabir press: Amirkabir University, pp. 1-286.
- Erban, L. E., Gorelick, S. M. and Zebker, H. A., 2014- groundwater extraction, land subsidence and sea-level rise in the Mekong Delta, Vietnam, pp. 1-5.
- Ferretti, A., Monti-Guarnieri, A., Prati, C., Rocca, F. and Massonet, D., 2007- InSAR principles-guidelines for SAR interferometry processing and interpretation vol. 19.
- Hayashi, T., Tokunaga, T., Aichi, M., Shimada, J. and Taniguchi, M., 2009- Effects of human activities and urbanization on groundwater environments: an example from the aquifer system of Tokyo and the surrounding area, *Science of the total environment*, vol. 407, pp. 3165-3172.
- Leake, S. A. and Galloway, D. L., 2010- Use of the SUB-WT Package for MODFLOW to simulate aquifer-system compaction in Antelope Valley, California, USA, in *Land Subsidence, Associated Hazards and the Role of Natural Resources Development: Proceedings of the Eighth International Symposium on Land Subsidence: Queretaro, Mexico*, International Association of Hydraulic Sciences, pp. 61-67.
- Mahmoodpour, M., Khamsehchiyan, M., Nikudel, M. R. and Ghassemi, M. R., 2015- Numerical simulation and prediction of regional land subsidence caused by groundwater exploitation in the southwest plain of Tehran, Iran, *Journal of Engineering Geology*, vol. 201, 6-28.
- Molaei, M., Meshkat, T., Akbari, K., Nazarjani, M., Esmailzadeh Nasiri, M. and Hesami, A., 2016 - Report of water resources' management of Tehran, Iran Water Resources Management Company, chapters 1-6.
- Phien-Wej, N., Giao, P. and Nutalaya, P., 2006- Land subsidence in Bangkok, Thailand, *Engineering geology*, vol. 82, pp. 187-201.
- Roustaei, M., 2016- considering the subsidence of Tehran Province, presented at the Conference of land subsidence phenomena (GSI), Iran.
- Sun, H., Grandstaff, D. and Shagam, R., 1999- Land subsidence due to groundwater withdrawal: potential damage of subsidence and sea level rise in southern New Jersey, USA, *Environmental Geology*, vol. 37, pp. 290-296.
- Tosi, L., Teatini, P. Carbognin, L. and Brancolini, G., 2009- Using high resolution data to reveal depth-dependent mechanisms that drive land subsidence: the Venice coast, Italy, *Tectonophysics*, vol. 474, pp. 271-284.